JACS
JOURNAL OF THE AMERICAN CHEMICAL SOCIETY
Communication
pubs.acs.org/JACS

CO_2 Reduction Catalyzed by Mercaptopteridine on Glassy Carbon

Dongmei Xiang, Donny Magana, and R. Brian Dyer*

Department of Chemistry, Emory University, Atlanta, Georgia 30322, United States

Supporting Information

ABSTRACT: The catalytic reduction of CO_2 is of great current interest because of its role in climate change and the energy cycle. We report a pterin electrocatalyst, 6,7-dimethyl-4-hydroxy-2-mercaptopteridine (PTE), that catalyzes the reduction of CO_2 and formic acid on a glassy carbon electrode. Pterins are natural cofactors for a wide range of enzymes, functioning as redox mediators and C1 carriers, but they have not been exploited as electrocatalysts. Bulk electrolysis of a saturated CO_2 solution in the presence of the PTE catalyst produces methanol, as confirmed by gas chromatography and ^{13}C NMR spectroscopy, with a Faradaic efficiency of 10−23%. FTIR spectroelectrochemistry detected a progression of two-electron reduction products during bulk electrolysis, including formate, aqueous formaldehyde, and methanol. A transient intermediate was also detected by FTIR and tentatively assigned as a PTE carbamate. The results demonstrate that PTE catalyzes the reduction of CO_2 at low overpotential and without the involvement of any metal.

The catalytic reduction of CO_2 is of great current interest. CO_2 is a potent greenhouse gas, and its anthropogenic emission has accelerated as global energy demand has increased. The current atmospheric CO_2 level of over 400 ppm has been implicated as the primary source of climate forcing, leading to calls for the development of a carbon-neutral energy cycle.[1,2] A sustainable approach to recycling CO_2 back to fuels will require the development of an efficient approach for its reduction using renewable energy sources such as solar energy. CO_2 is a very stable molecule, however, and its direct reduction is slow and requires a high overpotential.[3,4] The single-electron reduction of CO_2 encounters a large barrier due to the reorganization energy required to bend the stable linear molecule to produce the radical anion.[5,6]

This problem has spurred significant research to develop electrochemical[7−10] or photochemical[11−16] catalysts for efficient CO_2 reduction. Catalyst development has primarily focused on metals and metal complexes. Various metals including Pt, Au, Zn, and Fe have been reported to catalyze CO_2 reduction, primarily to the two-electron reduction products CO and formate.[7] Molecular catalysts based on polypyridyl complexes of Ru and Re have been developed, with labile ligand sites to coordinate a CO_2 molecule.[12,17] All of these approaches suffer from the need for high overpotentials to achieve reduction of CO_2.

Inspired by the role of pterin in biological catalysis, we have explored the use of 6,7-dimethyl-4-hydroxy-2-mercaptopteridine (PTE) (Figure 1a) as an electrocatalyst for CO_2 reduction. In water, PTE is predominately in the keto form (Figure 1a, right structure) as indicated by its FTIR spectrum. Pterins are natural cofactors for a wide range of enzymes, functioning as redox mediators and C1 carriers. In its biologically active form, the pyrazine ring is fully reduced

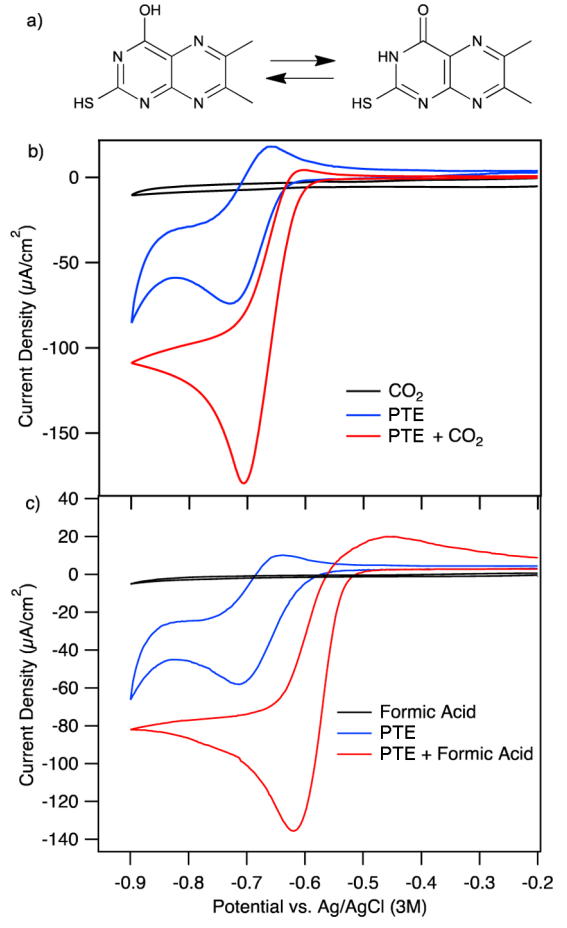

Figure 1. PTE electrocatalysis. (a) Equilibrium structures of PTE. (b) Cyclic voltammograms of saturated CO_2 solutions with (red) and without (black) PTE catalyst on a glassy carbon electrode. PTE alone under Ar is shown for comparison (blue). Conditions: 10 mM PTE, 100 mM KCl, 100 mM phosphate buffer (pH 6.3), scan rate of 1 mV/s. (c) Cyclic voltammograms of 33 mM formic acid with (red) and without (black) PTE on a glassy carbon electrode in 100 mM KCl solution at pH 4.6 and 4.2, respectively.

Received: August 7, 2014
Published: September 26, 2014

   dx.doi.org/10.1021/ja5081103 | J. Am. Chem. Soc. 2014, 136, 14007−14010

(H_4-PTE), and C1 substituents are carried at N5 of the pyrazine ring. Pterin generally acts as a two-electron reductant, transferring the electrons as hydride.[18] Methanogenesis in archaeal anaerobes depends on pterin cofactors such as methanopterin (MPT). C1 is loaded onto N5 of the reduced MPT as a formyl group and then converted to a cyclic methylene intermediate and finally a methyl group. Critical steps along this pathway have been shown to occur with the MPT cofactor alone and no enzyme present, although the initial steps usually involve a separate C1 carrier.[19,20] Thus, MPT has been shown to condense with formaldehyde to produce the N5-formyl derivative, which in turn cyclizes to form the CH_2-N5MPT intermediate on the route to forming methanol or methane. Furthermore, the active (reduced) form of pterin can be produced electrochemically.[21] These characteristics make pterin a promising candidate as an electrocatalyst for CO_2 reduction.

We observed reduction of CO_2 catalyzed by PTE at low overpotential on a glassy carbon electrode without the involvement of any metals. Electrochemical measurements were performed using a Reference 3000 potentiostat (Gamry Instruments). The working electrode was polished consecutively with 1 μm and then 0.05 μm alumina and sonicated before use. The electrochemistry of PTE on glassy carbon in buffer solution purged with Ar gas is quasi-reversible with a two-electron redox couple centered at −0.68 V vs Ag/AgCl, as shown in Figure 1b (blue curve). In contrast, when the solution is saturated with CO_2, a catalytic wave indicating CO_2 reduction is observed (red curve), characterized by significantly greater current flow and irreversible reduction (Figure 1b). CO_2 reduction does not occur in the absence of PTE (black curve). A catalytic reduction wave is also observed for formic acid in the presence of PTE, as shown in Figure 1c. No reduction of formic acid is observed without the PTE catalyst (Figure 1c, black trace). These results suggest that PTE can act as a single, multifunctional catalyst for successive two-electron reduction steps of CO_2, i.e., from CO_2 to formic acid and then to formaldehyde or further reduced products.

The products of CO_2 reduction were determined in bulk electrolysis using a reticulated vitreous carbon (RVC) electrode as the working electrode. Following bulk electrolysis of a saturated CO_2 solution containing the PTE catalyst in 100 mM KCl at pH 6.3 (100 mM phosphate buffer) for ~2 h at −0.65 V (vs Ag/AgCl), the products were detected by gas chromatography and ^{13}C NMR spectroscopy. Both methods demonstrated that methanol is formed in bulk electrolysis of a saturated CO_2 solution, whereas it is not detected when the solution is purged with Ar gas or in the absence of the PTE catalyst (Figures S1 and S2 in the Supporting Information). For bulk electrolysis of a $^{13}CO_2$ saturated solution, the ^{13}C NMR spectrum (Figure S2) shows peaks at 48 and 171 ppm due to ^{13}C-enriched methanol and formate, respectively, demonstrating that the origin of these products is from CO_2 reduction. The concentration of methanol produced was determined by GC analysis (Figure S3), which indicated that the Faradaic efficiency of methanol formation is between 10−23%. Formate and formaldehyde are the other major reduction products detected by IR and ^{13}C NMR spectroscopy, but these could not be quantified by the GC method.

The progress of the electrocatalytic reaction was followed using FTIR spectroelectrochemistry by flowing the sample solution from the electrochemical cell into an infrared transmission cell during bulk electrolysis. Figure 2 shows the

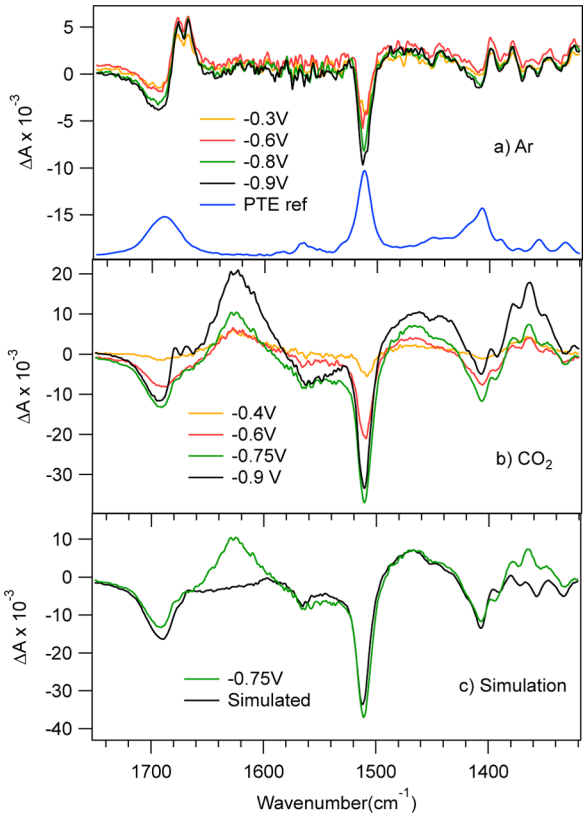

Figure 2. FTIR analysis of bulk electrolysis reactions (scan rate of 1 mV/s, RVC working electrode). (a, b) Difference FTIR spectra (spectra at indicated potentials minus the spectrum at no applied potential) of PTE under (a) Ar and (b) saturated CO_2 solutions scanned at 1 mV/s. (c) Simulated spectrum from reference spectra in D_2O. Spectra were acquired on a Varian 3100 FTIR spectrometer (50 μm path length CaF_2 cell, 2 cm^{-1} resolution) using LabVIEW to synchronize bulk electrolysis and FTIR data collection.

FTIR difference spectra (spectra at indicated potentials minus the spectrum at no applied potential) of PTE under (a) Ar or (b) CO_2 atmosphere and (c) the simulated spectrum using reference spectra of the products. Reduction of PTE under Ar (Figure 2a) leads to a progressive bleach of the ground-state bands (the unreduced spectrum is shown for comparison) as the potential is scanned more negative. A concomitant buildup of positive features is also observed, all shifted to lower frequency, characteristic of pterin reduction.[22] It should be noted that the ketone absorbance at 1690 cm^{-1} is only slightly shifted upon reduction (to 1679 cm^{-1}), whereas the pyrazine C═N mode at 1512 cm^{-1} disappears. This result is consistent with a two-electron reduction of the pyrazine ring, as expected from previous electrochemical studies.[21] When the same experiment is repeated with a saturated CO_2 solution (Figure 2b), as the potential becomes more negative a progression of new peaks due to the reduction of CO_2 is observed. At −0.40 V, the bleach features due to reduction of PTE are present, but the corresponding positive peaks are missing, indicating that the reduced PTE reacts rapidly with CO_2 and is not detected on the 1−2 min time scale of the FTIR experiment. We simulated the IR difference spectra using a linear combination of reference spectra of the products in D_2O and subtracting the initial PTE spectrum, as shown in Figure 2c. The simulated spectrum at −0.75 V gives the best fit with a formate:formaldehyde:methanol product ratio of 2:1.5:1. All of the major

dx.doi.org/10.1021/ja5081103 | J. Am. Chem. Soc. 2014, 136, 14007−14010

absorbances of formate (1350 and 1370 cm^{-1}), formaldehyde (1442 cm^{-1}), and methanol (1466 cm^{-1}) are well-fit by this procedure. The simulation does not account for several peaks, the most prominent at 1625 cm^{-1}, that are present throughout the reaction. We postulate that these features are due to a PTE-carbamate intermediate formed by addition of CO_2 to one of the nitrogens of the reduced pyrazine ring, by analogy to the IR spectra of known carbamates.[23] Buildup of the reduced PTE is also observed at the lowest potential (−0.9 V), as evidenced by the appearance of the positive peak at 1679 cm^{-1} (the ketone absorbance of two-electron-reduced PTE). Reduced PTE may accumulate at this potential as a result of faster catalysis and depletion of CO_2 in the solution.

Comparison of the present results with previous work using pyridinium in water to catalyze the reduction of CO_2 to methanol provides additional mechanistic insight.[24−26] The Bocarsly group observed CO_2 reduction to methanol on a Pt electrode with low overpotential.[25] They proposed a multistep mechanism in which pyridinium works as a one-electron shuttle, with the initial reduction of pyridinium to form the pyridinyl radical anion followed by reaction with CO_2 to form the carbamate adduct. This mechanism was questioned by another study that observed no methanol production, only competitive proton reduction.[26] Theoretical work also noted several problems, including a pK_a of ∼27 for the deprotonation of the pyridinyl radical in water, presenting a high energy barrier to the formation of the carbamate intermediate,[27,28] and a discrepancy between the calculated and observed redox potentials of the pyridinium/pyridinyl couple.[28−30] Alternative mechanisms have been proposed that involve surface interactions of pyridinium with the Pt electrode[29] or a surface-bound dihydropyridine species.[31,32] Finally, the MacDonnell group reported that pyridinium catalyzes CO_2 reduction in concert with a Ru or Re photosensitizer without the presence of a metal electrode.[16,24] Therefore, the role of the metal electrode in these reactions remains unclear.

We conclude that the mechanism of PTE catalysis is fundamentally different from that of pyridinium. Clearly no metal is involved in the reduction reactions on glassy carbon. The detection of two-electron-reduced PTE and a transient intermediate formed with CO_2 (likely a carbamate) indicates that the catalyst can act as a two-electron reductant and C1 carrier. The only products detected are formate, formaldehyde, and methanol, consistent with successive two-electron reduction steps. The difference in mechanism is due in part to different electrochemical behavior of the catalysts, which is evident from a comparison of the cyclic voltammograms of pyridinium and PTE on platinum, gold, and glassy carbon electrodes (Figure S5). Pyridinium shows a quasi-reversible redox reaction on a Pt electrode under Ar, but it does not show an oxidation wave on gold or any redox reactions on a glassy carbon electrode. Pt has a significantly lower hydrogen overpotential than the other electrodes, and therefore, the reduction of protons is competitive with the reduction of the pyridinium catalyst. This results in ample hydrogen atoms adsorbed on the electrode surface that can react with surface species, which may play a role in pyridinium catalysis on Pt. Glassy carbon has a high overpotential for proton reduction, and no reaction is observed with pyridinium. In contrast, the PTE catalyst shows quasi-reversible redox chemistry under Ar on all three of these electrodes, indicating that its redox chemistry is not necessarily coupled to proton reduction. Furthermore, it reduces CO_2 on glassy carbon under conditions where competitive reduction of protons is not an issue. The observed mechanism is consistent with the known ability of reduced pterins to catalyze two-electron reductions via hydride transfer to C1 substrates.

In summary, PTE acts as a molecular electrocatalyst for CO_2 reduction on a glassy carbon electrode. Gas chromatography and NMR and FTIR spectroscopy provide evidence of two-electron reduction of the PTE catalyst and reaction with CO_2 to form an intermediate species that is likely a PTE-carbamate, followed by successive two-electron reductions to formate, formaldehyde, and methanol. The efficiency of methanol production is modest, but it is worth noting that the PTE catalyst lacks the extended substituent at position 6 of the pyrazine ring normally present in methanogenic cofactors such as MPT.[19] Consequently, PTE cannot stabilize a cyclic methylene intermediate, which may limit the efficiency of further reduction steps beyond the first two-electron reduction to formate. We are currently exploring pterin derivatives that better mimic MPT as a means to improve the overall efficiency.

■ ASSOCIATED CONTENT

Supporting Information

GC and ^{13}C NMR product analysis (Figures S1−S3), FTIR reference spectra (Figure S4), and cyclic voltammogram comparisons (Figure S5). This material is available free of charge via the Internet at http://pubs.acs.org.

■ AUTHOR INFORMATION

Corresponding Author

briandyer@emory.edu

Notes

The authors declare no competing financial interest.

■ ACKNOWLEDGMENTS

This work was supported by the NSF through Grant DMR-1409851 (R.B.D.).

■ REFERENCES

(1) Hansen, J.; Sato, M.; Ruedy, R.; Nazarenko, L.; Lacis, A.; Schmidt, G. A.; Russell, G.; Aleinov, I.; Bauer, M.; Bauer, S.; Bell, N.; Cairns, B.; Canuto, V.; Chandler, M.; Cheng, Y.; Del Genio, A.; Faluvegi, G.; Fleming, E.; Friend, A.; Hall, T.; Jackman, C.; Kelley, M.; Kiang, N.; Koch, D.; Lean, J.; Lerner, J.; Lo, K.; Menon, S.; Miller, R.; Minnis, P.; Novakov, T.; Oinas, V.; Perlwitz, J.; Perlwitz, J.; Rind, D.; Romanou, A.; Shindell, D.; Stone, P.; Sun, S.; Tausnev, N.; Thresher, D.; Wielicki, B.; Wong, T.; Yao, M.; Zhang, S. *J. Geophys. Res.: Atmos.* **2005**, *110*, No. D18104.

(2) Hansen, J.; Sato, M.; Russell, G.; Kharecha, P. *Philos. Trans. R. Soc., A* **2013**, *371*, No. 20120294.

(3) Jitaru, M.; Lowy, D. A.; Toma, M.; Toma, B. C.; Oniciu, L. *J. Appl. Electrochem.* **1997**, *27*, 875−889.

(4) Kumar, B.; Llorente, M.; Froehlich, J.; Dang, T.; Sathrum, A.; Kubiak, C. P. *Annu. Rev. Phys. Chem.* **2012**, *63*, 541−569.

(5) Kafafi, Z. H.; Hauge, R. H.; Billups, W. E.; Margrave, J. L. *Inorg. Chem.* **1984**, *23*, 177−183.

(6) Yoshioka, Y.; Jordan, K. D. *Chem. Phys. Lett.* **1981**, *84*, 370−374.

(7) Hori, Y. *Mod. Aspects Electrochem.* **2008**, *42*, 89−189.

(8) Kondratenko, E. V.; Mul, G.; Baltrusaitis, J.; Larrazabal, G. O.; Perez-Ramirez, J. *Energy Environ. Sci.* **2013**, *6*, 3112−3135.

(9) Costentin, C.; Robert, M.; Savéant, J.-M. *Chem. Soc. Rev.* **2013**, *42*, 2423−2436.

(10) Oh, Y.; Hu, X. *Chem. Soc. Rev.* **2013**, *42*, 2253−2261.

(11) Morris, A. J.; Meyer, G. J.; Fujita, E. *Acc. Chem. Res.* **2009**, *42*, 1983−1994.

(12) Benson, E. E.; Kubiak, C. P.; Sathrum, A. J.; Smieja, J. M. *Chem. Soc. Rev.* **2009**, *38*, 89−99.
(13) Ikeue, K.; Yamashita, H.; Anpo, M.; Takewaki, T. *J. Phys. Chem. B* **2001**, *105*, 8350−8355.
(14) Dhakshinamoorthy, A.; Navalon, S.; Corma, A.; Garcia, H. *Energy Environ. Sci.* **2012**, *5*, 9217−9233.
(15) Mao, J.; Li, K.; Peng, T. Y. *Catal. Sci. Technol.* **2013**, *3*, 2481−2498.
(16) Boston, D. J.; Pachón, Y. M. F.; Lezna, R. O.; de Tacconi, N. R.; MacDonnell, F. M. *Inorg. Chem.* **2014**, *53*, 6544−6553.
(17) Dubois, M. R.; Dubois, D. L. *Acc. Chem. Res.* **2009**, *42*, 1974−1982.
(18) Keltjens, J. T.; Vanderdrift, C. *FEMS Microbiol. Lett.* **1986**, *39*, 259−303.
(19) Dimarco, A. A.; Bobik, T. A.; Wolfe, R. S. *Annu. Rev. Biochem.* **1990**, *59*, 355−394.
(20) Maden, B. E. H. *Biochem. J.* **2000**, *350*, 609−629.
(21) Dryhurst, G.; Raghavan, R.; Egeserpkenci, D.; Karber, L. G. *Adv. Chem. Ser.* **1982**, *201*, 457−487.
(22) Moore, J.; Wood, J. M.; Schallreuter, K. U. *Biochemistry* **1999**, *38*, 15317−15324.
(23) Hisatsune, C. *Can. J. Chem.* **1984**, *62*, 945−948.
(24) Boston, D. J.; Xu, C. D.; Armstrong, D. W.; MacDonnell, F. M. *J. Am. Chem. Soc.* **2013**, *135*, 16252−16255.
(25) Cole, E. B.; Lakkaraju, P. S.; Rampulla, D. M.; Morris, A. J.; Abelev, E.; Bocarsly, A. B. *J. Am. Chem. Soc.* **2010**, *132*, 11539−11551.
(26) Costentin, C.; Canales, J. C.; Haddou, B.; Savéant, J.-M. *J. Am. Chem. Soc.* **2013**, *135*, 17671−17674.
(27) Keith, J. A.; Carter, E. A. *J. Am. Chem. Soc.* **2012**, *134*, 7580−7583.
(28) Lim, C. H.; Holder, A. M.; Musgrave, C. B. *J. Am. Chem. Soc.* **2013**, *135*, 142−154.
(29) Ertem, M. Z.; Konezny, S. J.; Araujo, C. M.; Batista, V. S. *J. Phys. Chem. Lett.* **2013**, *4*, 745−748.
(30) Yan, Y.; Gu, J.; Bocarsly, A. B. *Aerosol Air Qual. Res.* **2014**, *14*, 515−521.
(31) Keith, J. A.; Carter, E. A. *Chem. Sci.* **2013**, *4*, 1490−1496.
(32) Keith, J. A.; Carter, E. A. *J. Phys. Chem. Lett.* **2013**, *4*, 4058−4063.